An optimal vibration control logic for minimising fatigue damage in flexible structures

P. Ambrosio, G. Cazzulani, F. Resta, F. Ripamonti *

Politecnico di Milano, Mechanical Engineering Department, Via La Masa 1, 20156 Milano, Italy

Received 17 May 2013
Received in revised form
18 October 2013
Accepted 1 November 2013
Handling Editor: D.J. Wagg
Available online 3 December 2013

1. Introduction

Vibration control and fatigue damage problems have usually been considered separately during structure design. The former is usually managed as a dynamics problem, and aims to minimise vibrations in terms of displacement or noise, while the fatigue phenomenon is typically taken as a structural problem. Moreover, in vibration control applications, it is generally held that vibration reduction would intrinsically reduce fatigue damage in structures. Although this may be generally true, there are some examples in which this assumption is no longer valid. This is the case, for example, with high performance control logics that apply high control forces to reduce significantly structure vibrations, with consequent local damage effects. Other examples could be found in conditions where low displacement vibrations hide high structure stresses, or in applications showing significant spillover problems. Moreover, even if on a particular application a vibration control would improve structure life, this does not mean that it is the best solution from a fatigue point of view and probably the control logic could be further improved to minimise fatigue damage.

For these issues, the scientific literature provides few applications. A contribution from Ray et al. [1] pointed out that a significant improvement in service life could be achieved by a small reduction in the system's dynamic performance, taking the material model into account the control design. In any case, the research field did not offer relevant developments. On the other hand, control logics aiming to extend structure life have some applications on large mechanical structures where their results could be highly cost-effective. This is the case with steel jacket platforms, where control mechanisms designed

* Corresponding author. Tel.: +39 0223998480; fax: +39 0223998492.
E-mail address: francesco.ripamonti@polimi.it (F. Ripamonti).

to increase fatigue life are preferable to simple deck displacement control [2]. Recently, with the increased use of wind energy, wind turbine fatigue has been investigated in depth. The wind industry seeks to design wind turbines maximizing energy production and increasing fatigue life. To achieve this, the research community is asked to design wind turbines that can extract maximum energy while reducing component and system loads. As turbines become larger and more flexible, it is increasingly important not only to consider the effect of the controller on component loads, but also to design the controller with load reduction as a part of the primary objective [3–5]. A last example about fatigue control has been presented by Chomette et al. in 2010 [6]. They proposed an active logic for the damage reduction of printed circuit boards by means of piezoelectric actuators and sensors.

However, the design of control architectures that take fatigue into account is limited to these very particular applications, and the control logics developed lack of general application. Hence, the aim of this paper is to investigate the fatigue and vibration problem as an integrated one and develop a control logic that takes into account fatigue damage on the structure. The problem has been theoretically analysed, and a solution proposed that could be widely applied in vibration control applications. The study starts by considering a model of fatigue damage in the frequency domain for control formulation (Section 2). Then an adaptive control algorithm for fatigue minimization is introduced. This logic, based on the optimal control theory, is designed to take into account structural damage directly in the cost function (Section 3). Finally the control solution proposed is validated both numerically and experimentally (Section 4).

2. Frequency domain formulation of fatigue damage

Consider the state-space model of a generic linear system

$$\dot{\mathbf{x}} = [\mathbf{A}]\mathbf{x} + [\mathbf{B}]\mathbf{u_c} + \mathbf{w_d} \tag{1a}$$

$$\mathbf{y} = [\mathbf{C}]\mathbf{x} + [\mathbf{D}]\mathbf{u_c} + \mathbf{w}_n \tag{1b}$$

where $\mathbf{x}$ is the $n \times 1$ state variable vector, $\mathbf{y}$ is the $n_s \times 1$ measured output vector and $\mathbf{u_c}$ is the $n_a \times 1$ control action vector. Moreover, $[\mathbf{A}]$ is the $n \times n$ state matrix, $[\mathbf{B}]$ is the $n \times n_a$ control input matrix, $[\mathbf{C}]$ is the $n_s \times n$ observation matrix, while $\mathbf{w_d}$ and $\mathbf{w}_n$ are respectively the input and measurement noise vectors.

In many practical applications both $\mathbf{w_d}$ and $\mathbf{w}_n$ are unknown and they are not considered either for optimal actuator and sensor positioning or in control law synthesis. Indeed, considering the system as strictly proper ($[\mathbf{D}] = [\mathbf{0}]$) Eq. (1) can be written as

$$\dot{\mathbf{x}} = [\mathbf{A}]\mathbf{x} + [\mathbf{B}]\mathbf{u_c} \tag{2a}$$

$$\mathbf{y} = [\mathbf{C}]\mathbf{x} \tag{2b}$$

When the system is a controlled continuous structure, state variable cardinality tends to be infinite. For this reason, for our purposes and without sacrificing generality, the structure is modelled applying a modal coordinates truncation [7], which is considered to be consistent with the frequency range investigated. According to this assumption and considering only m modes, the state-space vector in (2) becomes

$$\mathbf{x}(t) = \begin{bmatrix} q_1(t) \\ \vdots \\ q_m(t) \\ \dot{q}_1(t) \\ \vdots \\ \dot{q}_m(t) \end{bmatrix} = \begin{bmatrix} \mathbf{q}_r(t) \\ \dot{\mathbf{q}}_r(t) \end{bmatrix} \tag{3}$$

where q_i is the i-th modal coordinate, describing the structure's dynamics.

In order to compute the fatigue damage, the displacement should be written in physical coordinates. Let ξ be the physical coordinate of a generic point along the structure and $z(\xi, t)$ its physical displacement. According to the definition of modal transformation

$$z(\xi, t) \simeq \mathbf{\Phi}_r^T(\xi)\mathbf{q}_r(t) \tag{4}$$

where $\mathbf{\Phi}_r(\xi)$ is the eigenvector matrix of the truncated model evaluated at ξ. For this analysis it is important to point out that, according to the modal approach, the structure vibration is written as a product of a first part $\mathbf{\Phi}_r$, which is a function only of the position, and a second part $\mathbf{q}_r$, which is a function only of time. Consequently, noting the assumption of structure linearity, the stress tensor is written as

$$[\boldsymbol{\sigma}](\xi, t) = \sum_{i=1}^{m} [\tilde{\boldsymbol{\sigma}}_i](\xi) q_i(t) \tag{5}$$

where $[\boldsymbol{\sigma}]$ is the 3×3 stress tensor in ξ and at time t and $[\tilde{\boldsymbol{\sigma}}_i]$ is the stress tensor in ξ due to a unitary displacement of the i-th modal coordinate. Again, $[\tilde{\boldsymbol{\sigma}}_i]$ depends only on the modal analysis and therefore can be identified in advance.

Once the stress tensor is known, fatigue damage can be computed through an appropriate equivalent stress σ_{eq} [8,9], the *S–N* curves [10] and Miner's rule [11,12].

Among all the various equivalent stress formulations present in the scientific literature, consider for example, without sacrificing generality, the Sines method [13]. This is based on the maximum deviatory deformation energy and it is written as a nonlinear function of $[\sigma]$ as

$$\sigma_{eq}(\xi,t)=\frac{1}{1-\frac{\sigma_{11,m}+\sigma_{22,m}+\sigma_{33,m}}{R_m}}\sqrt{\sigma_{11,a}^2+\sigma_{22,a}^2+\sigma_{33,a}^2-\sigma_{12,a}\sigma_{23,a}-\sigma_{12,a}\sigma_{13,a}-\sigma_{23,a}\sigma_{13,a}} \tag{6a}$$

$$=f_{eq}\left(\sum_{i=1}^{m}[\tilde{\sigma}_i](\xi)q_i(t)\right)=f_{eq}([\sigma](\xi,t)) \tag{6b}$$

with

$$[\sigma]=[\sigma_a]+[\sigma_m]=\begin{bmatrix}\sigma_{11,a} & \sigma_{12,a} & \sigma_{13,a}\\ \sigma_{12,a} & \sigma_{22,a} & \sigma_{23,a}\\ \sigma_{13,a} & \sigma_{23,a} & \sigma_{33,a}\end{bmatrix}+\begin{bmatrix}\sigma_{11,m} & \sigma_{12,m} & \sigma_{13,m}\\ \sigma_{12,m} & \sigma_{22,m} & \sigma_{23,m}\\ \sigma_{13,m} & \sigma_{23,m} & \sigma_{33,m}\end{bmatrix} \tag{7}$$

where the footer *a* refers to the harmonic part of the tensor and *m* to the average one.

In order to go deeper into the analysis, the stress tensor in the frequency domain needs to be evaluated. Therefore, applying the Fourier transformation, Eq. (5) becomes

$$[\mathbf{\Sigma}](\xi,j\omega)=\sum_{i=1}^{m}[\tilde{\sigma}_i](\xi)Q_i(j\omega) \tag{8}$$

where $[\mathbf{\Sigma}]$ and $Q_i\in\mathbb{C}$ are the frequency domain transforms of $[\sigma]$ and q_i. With regard to Eq. (8) it can be pointed out that

- the expression is completely general and the only assumption is the linearity of the structure;
- since $[\tilde{\sigma}_i]$ does not depend on time *t*, it is considered as a constant in the Fourier integral.

Hence, according to Eq. (6)

$$|\Sigma_{eq}(\xi,\omega)|=f_{eq}(|[\mathbf{\Sigma}](\xi,\omega)|)=f_{eq}\left(\left|\sum_{i=1}^{m}[\tilde{\sigma}_i](\xi)Q_i(j\omega)\right|\right) \tag{9}$$

where $|\cdot|$ denotes the amplitude operator of a given complex value.

Once $|\Sigma_{eq}(\xi,\omega)|$ is computed, the *S–N* curve can be introduced and the structure life in terms of the number of cycles can be found. This curve expresses the relationship between the limit number of cycles before failure and the cyclic stress amplitude. According to [10], the equation of the *S–N* curve (Fig. 1) is generically written as

$$\log_{10}(N)=\log_{10}(a_1)-b_1\log_{10}(\Sigma_{eq}) \quad \text{for } \Sigma_{eq}\geq\Sigma_{lim} \tag{10a}$$

$$\log_{10}(N)=\log_{10}(a_2)-b_2\log_{10}(\Sigma_{eq}) \quad \text{for } \Sigma_{eq}<\Sigma_{lim} \tag{10b}$$

where (10a) refers to the solid line in Fig. 1 and (10b) refers to the dashed one, while a_1, a_2, b_1 and b_2 are constant scalars depending on the material and, finally, Σ_{lim} is the fatigue limit.

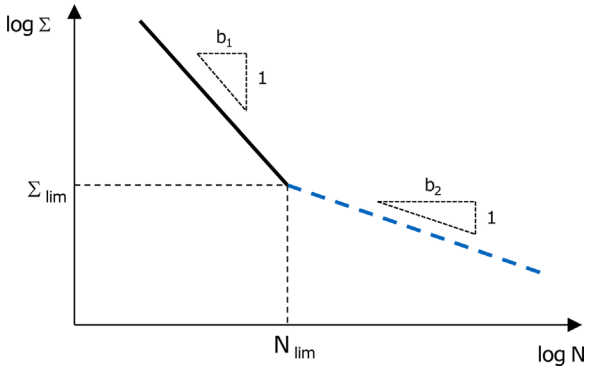

Fig. 1. Example of a *S–N* curve; Σ is the stress and *N* is the number of cycles at failure.

With simple calculations, the number of cycles before failure can be written as

$$N(\xi,\omega)=\frac{a_j}{|\Sigma_{\text{eq}}(\xi,\omega)|^{b_j}}=\frac{a_j}{[f_{\text{eq}}(|\sum_{i=1}^{m}[\tilde{\sigma}_i](\xi)Q_i(j\omega)|)]^{b_j}} \tag{11}$$

with j being equal to 1 or 2 whether the material is loaded with a stress higher or lower than the fatigue limit. Eq. (11) shows well the nonlinear behaviour of the fatigue damage:

- the equivalent stress is a nonlinear function of the stress tensor;
- the relationship between N and Σ is nonlinear;
- the S–N curve is discontinuous.

The fatigue damage due to a certain frequency ω can now be discussed. It is not directly affected by the frequency itself, but, given a fixed period of time ΔT, the number of load cycles is directly proportional to it

$$n(\omega)=\frac{\omega}{2\pi}\,\Delta T \quad [(\#\text{ cycles})] \tag{12}$$

Therefore, the damage can be easily computed using Miner's formula (based on the Palmgren-Miner linear damage hypothesis [11,12]) as

$$D(\xi,\omega)=\frac{n(\omega)}{N(\xi,\omega)}=\frac{\omega\Delta T}{2\pi N(\xi,\omega)} \tag{13}$$

where $D(\xi,\omega)$ is the damage accumulated during the ΔT period in the position ξ of the structure because of the vibration component at the frequency ω.

Introducing Eq. (11) into (13), the damage function becomes

$$D(\xi,\omega)=\begin{cases}\dfrac{\omega}{2\pi a_1\Delta T}\left[f_{\text{eq}}\left(\left|\sum_{i=1}^{m}[\tilde{\sigma}_i](\xi)Q_i(j\omega)\right|\right)\right]^{b_1} & \text{per } \Sigma_{\text{eq}}\geq\Sigma_{\text{lim}}\\ \dfrac{\omega}{2\pi a_2\Delta T}\left[f_{\text{eq}}\left(\left|\sum_{i=1}^{m}[\tilde{\sigma}_i](\xi)Q_i(j\omega)\right|\right)\right]^{b_2} & \text{per } \Sigma_{\text{eq}}<\Sigma_{\text{lim}}\end{cases} \tag{14}$$

Finally, the total damage can be computed integrating Eq. (14) as follows:

$$D(\xi)=\int_0^{+\infty}D(\xi,\omega)\,\mathrm{d}\omega \tag{15}$$

where $D(\xi)$ is the total damage cumulated in the time period ΔT in the position ξ of the structure.

Because of its complexity, Eq. (15), which takes into account the whole fatigue problem, cannot be directly used for control law synthesis. Nevertheless it represents an important milestone from which the following considerations can be drawn:

1. The damage $D(\xi,\omega)$ is directly proportional to the frequency ω. This means that, keeping constant all the other quantities (mode shapes, stress amplitude, etc.), the higher the structure load frequency, the higher the structure damage.
2. As shown in Fig. 1, the S–N curve slope above the fatigue limit is higher than below, i.e. $b_1<b_2$. Indeed, the damage induced by a load $\Sigma_{\text{eq}}\geq\Sigma_{\text{lim}}$ is significantly more important. For these reasons, a control law that aims to reduce fatigue damage should focus mainly on the oscillations with amplitude greater than the fatigue limit.
3. Whether modal displacements are normalized to the maximum modal shape physical displacement, the stress $[\tilde{\sigma}_i]$ proves monotone with the mode eigenfrequency. This is because higher frequency modes are characterized by higher modal shape complexity and consequently by more dangerous strains and stresses on the structure.
4. Although discussion has been generic, a hypothesis is needed for Eq. (15): each harmonic component of $[\boldsymbol{\Sigma}]$ contributes separately to the overall damage induced onto the structure. This means that each harmonic oscillation of the equivalent stress could be separately counted in Miner's method. In fact, to compute the number of fatigue cycles affecting the structure, counting methods such as the Rainflow are commonly used. However, Eq. (15) highlights the main parameters affecting the fatigue damage.

These considerations permit, as shown in the section below, synthesis of a suitable control logic for fatigue damage reduction.

3. The control algorithm

The aim of the control synthesis is to implement an optimal control problem [14,15] that reduces structure vibrations taking into account the fatigue issues introduced above. In fact, control design consists in the definition of the two matrices

[**Q**] and [**R**] of the generic quadratic functional

$$J_r = \int_0^\infty [\mathbf{x}^T[\mathbf{Q}]\mathbf{x} + \mathbf{u}_\mathbf{c}^T[\mathbf{R}]\mathbf{u}_\mathbf{c}]\,\mathrm{d}t \tag{16}$$

which can be solved with the well-known Continuous Algebraic Riccati Equation (CARE).

Below, the Fatigue Linear Quadratic Regulator (FLQR) is presented, initially as an optimal feedback control and then in its adaptive version, which extends its applicability to a wider number of cases.

3.1. Fatigue control logic

Starting from the considerations drawn in Section 2, since the control logic should not ignore the vibration control problem, the [**Q**] matrix has been designed as a sum of vibration [$\mathbf{Q}_v$] and fatigue [$\mathbf{Q}_f$] weighting matrices, i.e.

$$[\mathbf{Q}] = [\mathbf{Q}_v] + [\mathbf{Q}_f] \tag{17}$$

Secondly, the [**R**] matrix should ensure a consistent "minimum fuel" component in order to avoid high control forces and consequent local damage effects. Hence, from the [$\mathbf{R}_v$] matrix (considering only the vibration problem), the [**R**] has been designed as

$$[\mathbf{R}] = \rho_f[\mathbf{R}_v] \tag{18}$$

where ρ_f is a coefficient ensuring that for any [$\mathbf{Q}_f$]

$$\frac{\|\,\mathrm{diag}([\mathbf{Q}_v]+[\mathbf{Q}_f])\,\|_2}{\|\,\mathrm{diag}([\mathbf{R}])\,\|_2} = \mathrm{const} \tag{19}$$

where $\|\cdot\|_2$ operator represents the norm 2 of a vector.

Eq. (19) assumes a fundamental role in ensuring the "minimum fuel" component; whatever [$\mathbf{Q}_v$] and [$\mathbf{Q}_f$] are considered, the control force amplitude is limited.

Particular attention has to be paid on the matrix [$\mathbf{Q}_f$]. Assume that we know the Root Mean Square (rms) value of the generic i-th modal component

$$\overline{q}_i = \mathrm{rms}(q_i) = \frac{1}{T}\sqrt{\int_0^T q_i^2(t)\,\mathrm{d}t} \tag{20}$$

The proposed matrix in state-space form is

$$\mathbf{Q}_f = \begin{bmatrix} \mathbf{Q}_{fr} & \mathbf{O} \\ \mathbf{O} & \mathbf{Q}_{fr} \end{bmatrix} \tag{21}$$

where it is supposed to weight both modal velocity and displacement. The weighting matrix [$\mathbf{Q}_{fr}$] is computed as

$$\mathbf{Q}_{fr} = [\omega_{0,1}a_1, \ldots, \omega_{0,r}a_r]^T[\omega_{0,1}a_1, \ldots, \omega_{0,r}a_r] \tag{22}$$

where

$$a_i = \alpha\tilde{\sigma}_{\mathrm{eq},i}^{\max}\frac{\overline{q}_i}{\sum_{j=1}^r \overline{q}_j} \tag{23}$$

In Eq. (23):

- The constant α regulates the relative component of [$\mathbf{Q}_f$] and [$\mathbf{Q}_v$] on overall control, i.e. its value imposes if the control mainly acts as a vibration controller or for fatigue damage reduction.
- $\tilde{\sigma}_{\mathrm{eq},i}^{\max}$ is the maximum equivalent stress for the i-th modal shape. It takes into account that higher order modes correspond to higher stresses.
- The ratio $\overline{q}_i/\sum_{j=1}^r \overline{q}_j \in [0, 1]$ allows the control effort to be concentrated on the most stressed modes. In fact, it is equal to zero if $\overline{q}_i = 0$ and equal to one if $\overline{q}_j = 0$ for any $j \neq i$ and is an indicator of the disturbance frequency distribution along the controlled frequency band. Therefore, if $\overline{q}_i$ is greater than the other modal components the optimal control will focus on that mode.

Then, to complete the definition of [$\mathbf{Q}_{fr}$], each coefficient a_i is multiplied by $\omega_{0,i}$ (the i-th system natural frequency). Indeed, if for example the $\overline{q}_i$ and a_i of two modes were high compared to others, it would mean that the system is mainly excited by a disturbance with an harmonic component at those modes' frequencies. However, for the fatigue damage problem, the higher frequency mode will be more critical.

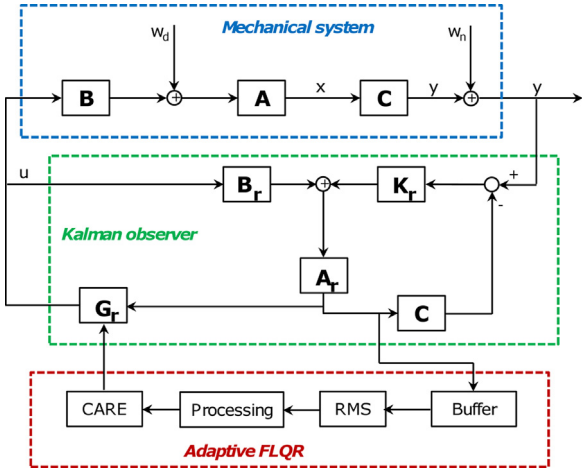

Fig. 2. The FLQR block diagram.

3.2. Adaptive fatigue control

The matrix $[\mathbf{Q}_f]$, defined in the previous section, is constructed on the hypothesis that the modal components rms $(\overline{q}_i)$ are known at the control design stage and do not change during the structure's life. However, this is not generally true and therefore an alternative solution is required. The proposed solution is an adaptive control logic [16]. In particular the adaptive version of fatigue control, whose complete block diagram is shown in Fig. 2, will be referred to as *Fatigue Linear Quadratic Regulator* (FLQR).

The modal state estimation of the system $q_i(t)$ is known as an output of the Kalman filter [17,18] and, therefore, it can be used to update, at a fixed time interval T_{update}, the modal coordinate rms values $(\hat{\overline{q}}_i = \text{rms}(\hat{q}_i)$ for any $i = 1, \ldots, m)$ and, consequently, the $[\mathbf{Q}_f]$ matrix. Finally, the control gains are computed solving the CARE. The feasibility of such a solution lies in an optimized algorithm that can solve the CARE in a relatively short computing time, if compared to the T_{update}, considering the disturbance characteristics and the model order.

Summarizing, for each time interval T_{update}, the FLQR logic performs the following operations:

- the state estimator observes and records the state variables $q_i(t)$ and, at the end of the time interval, it computes the modal components rms $(\overline{q}_i)$;
- the adaptive controller computes $[\mathbf{R}]$ and $[\mathbf{Q}]$, according to Eqs. (17)–(23), and performs the CARE optimization returning the new control gain matrix $[\mathbf{G}_r](k \cdot T_{\text{update}})$;
- because of the discontinuity of the control forces at the updating switch, the control matrix is changed only if the structure stress reaches a value higher than a limit threshold σ_0

$$\hat{\sigma}_{\max} = \sum_{i=1}^{m} \tilde{\sigma}_{\text{eq},i}^{\max} \hat{\overline{q}}_i > \sigma_0 \tag{24}$$

where $\hat{\sigma}_{\max}$ is an indicator of the stress intensity. It does not represent the actual maximum equivalent stress on the structure because firstly the maximum modal stresses for different modes are not in the same position on the structure and secondly the modal displacements may not be in phase. In any case, it represents a conservative approximation of the structure maximum stress.

An experimental validation of the control logic presented is reported in the following section.

4. Experimental validation

This section shows a brief description of the test rig and discusses the experimental validation and the performance of the FLQR control logic.

4.1. The test bench

A general view of the test bench is given in Fig. 3. It represents the two sides of the smart structure (a carbon fibre epoxy plate [19,20]) that was to be controlled with its actuators and sensor. The experiments involve a variety of devices and

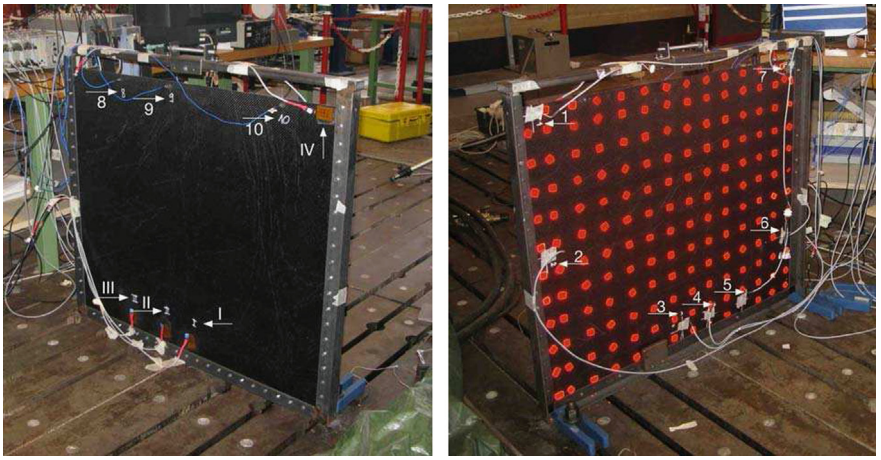

Fig. 3. The experimental test rig: piezoelectric patches and accelerometers on side 1 (left) and strain gauges on side 2 (right).

a complete description of the test rig elements is

1. *Carbon-fibre plate*: a 1.1×0.95 m carbon fibre epoxy plate, 1.4 mm thick and made up of seven parallel 0–90° ply layers.
2. *Frame*: a rectangular steel frame used to clamp the plate. It consisted of three *L* beams at the plate's clamped sides and a tubular beam in correspondence with the plate's free edge; a tensioning system was implemented on the tubular beam in order to introduce pre-tensioning in the system.
3. *Piezoelectric patches*: four patches, of which patches I, II and III (Fig. 3 on the left) were used to actuate the control while the fourth generated the disturbances.
4. *Strain gauges*: seven uniaxial strain gauges; strain gauges 1, 3, 4 and 5 (Fig. 3 on the right) were respectively co-located with piezoelectric patches IV, I, II and III, and were used simply as direct measurements for modal identification; strain gauges 2, 6 and 7 were used also for the control observer.
5. *Accelerometers*: three piezoelectric accelerometers used for the control logics observer and numbered as sensors 8, 9 and 10 (Fig. 3 on the left).

A detailed scheme of the whole experimental rig is shown in Fig. 4.

The control logics, developed on the experimental test bench, aimed to control the $[0, 50]$ Hz frequency band, corresponding to the first 9 modes, and to observe the first 15 modes.

System identification was effected by setting the Frequency Response Function (FRF) between the 4 inputs (piezoelectric patches) and the 10 outputs (accelerometers and strain gauges). This numerical model was adopted both for numerical tests and the implementation of the control logic.

The results are discussed in terms of both FRF and Rainflow counting methods [21–23].

4.2. FLQR results

As previously discussed, FLQR is an adaptive control logic that performs a control matrix update at fixed time intervals as a function of the measured oscillation amplitude of the system state. At the first time interval (when the control is switched on) the FLQR coincides with a classical Linear Quadratic Regulator (LQR) control logic, then it changes, setting up the vibration state of the structure and the fatigue damage minimization objective. In this way, the adaptive FLQR control was compared with LQR control.

During this experimental campaign the fatigue functional, defined in Section 3, requires knowledge of the maximum modal stresses ($\tilde{\sigma}_{\mathrm{eq},i}^{\max}$), i.e. the set of maximum stresses along the structure due to unitary displacement for each mode. Since the model used for the control synthesis was built using MIMO identification, the modal stresses were known only in correspondence with the strain gauge positions. Therefore, it was assumed that the maximum modal stress for each mode was registered on strain gauge 7 (Fig. 3 on the right). This assumption was proved with a structure FEM model.

In the following, two main tests with two different disturbances are analysed in detail:

1. a random noise over the $[0, 50]$ Hz frequency band (the overall range containing all the controlled modes);
2. a double harmonic disturbance at 10.5 and 48.1 Hz (corresponding to the 1st and 9th controlled modes).

These tests are presented in the sections below, and show how FLQR logic can reduce fatigue damage on the structure.

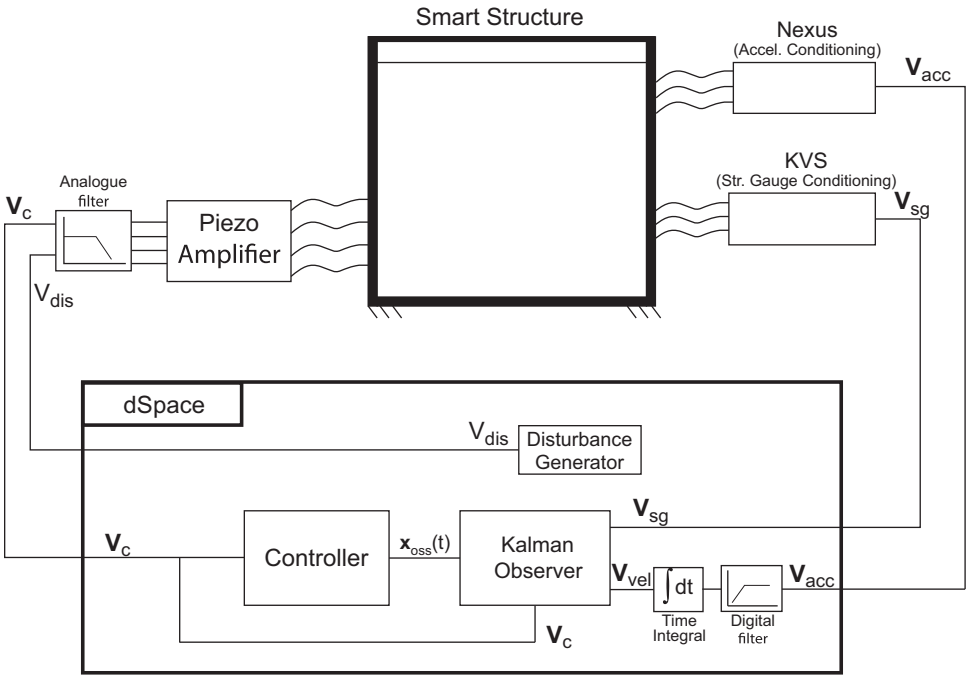

Fig. 4. The test rig scheme: structure, amplifiers and controller.

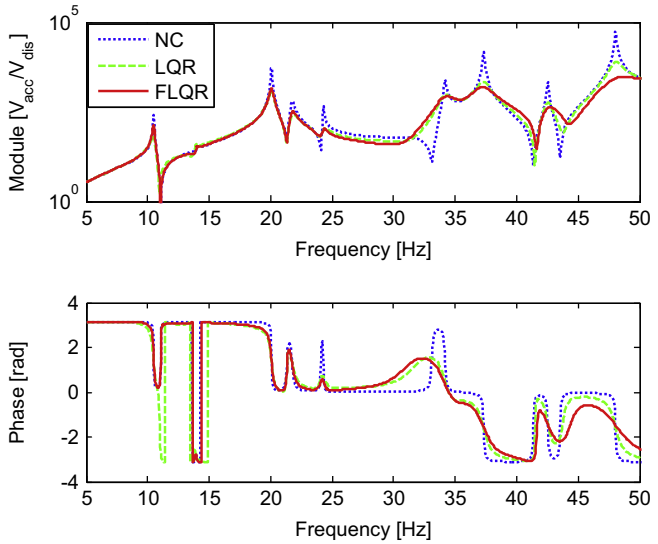

Fig. 5. Numerical FRF between the disturbance piezoelectric patch IV and accelerometer 8 for the following configurations: NC, LQR and FLQR for a Random Disturbance in the [0, 50] Hz frequency band (test 1).

4.3. Test 1: Random Disturbance

The first test performed during the experimental validation aimed to describe the system response to white noise random excitation over the whole controlled frequency band, i.e. [0, 50] Hz. The numerical and experimental results in terms of FRF between disturbance and accelerometer 8 are shown in Figs. 5 and 6 respectively.

To better explain the results, two main considerations, outlined in Section 3, should be recalled:

- higher order modes present higher modal stresses for equal maximum displacements;
- for equal stress oscillation amplitudes, the higher frequency ones are more dangerous in terms of structure fatigue life owing to the higher number of accumulated cycles.

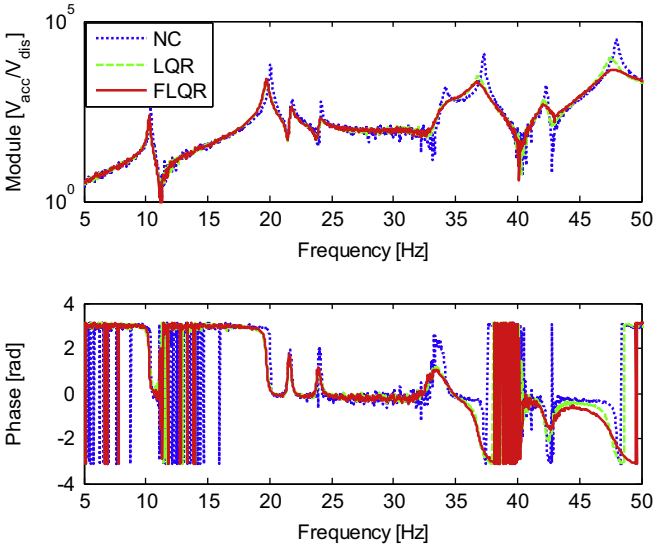

Fig. 6. Experimental FRF between the disturbance piezoelectric patch IV and accelerometer 8 for the following configurations: NC, LQR and FLQR for a Random Disturbance in the [0, 50] Hz frequency band (test 1).

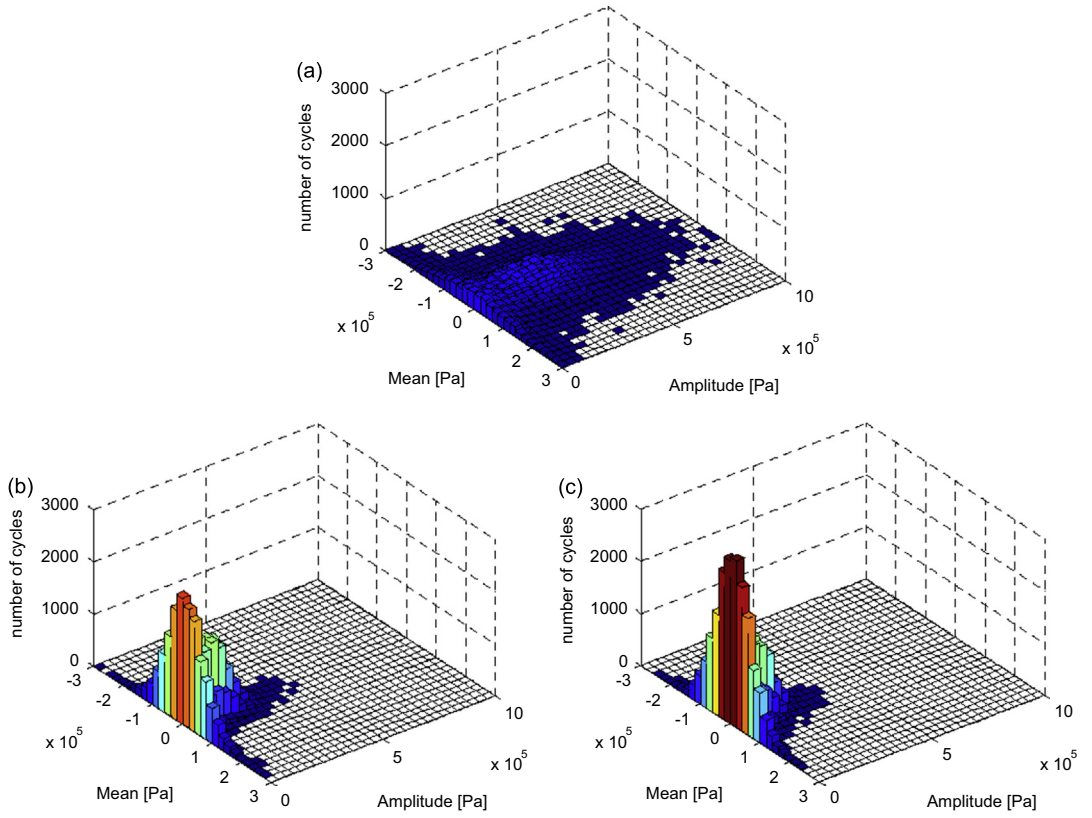

Fig. 7. Experimental Rainflow histogram (i.e. each bar represents the number of cycles associated to a certain amplitude and a mean value) for a [0, 50] Hz Random Disturbance (test 1) on NC (a), LQR (b) and FLQR (c) system.

From the figures it can be seen that FLQR relaxes control on the first modes and concentrates energy on the higher ones. This result shows one of the most important achievements of the proposed logic. It is confirmed by the values of the weight matrices Q_v (LQR) and Q (FLQR)

$$\mathrm{diag}(Q_v) = [0.4\ \ 0.4\ \ 0.4\ \ 0.4\ \ 0.4\ \ 0.4\ \ 0.4\ \ 0.4\ \ 0.4]$$

$$\mathrm{diag}(Q) = [2.0e-4 \;\; 4.0e-4 \;\; 2.7e-3 \;\; 1.5e-1 \;\; 1.7e2 \;\; 2.2e1 \;\; 6.2e1 \;\; 1.1e2 \;\; 3.9e2] \tag{25}$$

It is possible to notice that the most significant modes from the fatigue point of view are the 9th, the 8th and the 5th. The damping increase provided by FLQR on these modes is particularly evident in the phase diagram in Figs. 5 and 6.

Fig. 7 shows the Rainflow histograms for Not Controlled (NC), LQR and FLQR controlled systems. Each bar represents the number of cycles, in the whole time history, with given mean and amplitude stresses. The analysis highlights that LQR and FLQR logics reduce the number of higher amplitude cycles, and the FLQR histogram is almost null over 1.5 MPa. Switching from LQR to FLQR and applying almost the same control forces in terms of amplitude, the effect on structure fatigue life is notably improved.

These qualitative considerations are confirmed by the structure damage index computed using Miner's formula and the corresponding percentage improvement computed from NC to LQR and from LQR to FLQR (Table 1). In the table the damage analysis is reported for both the most critical point (strain gauge 7) and the average of all the strain gauges, and they are respectively denoted *Max Damage* and *Mean Damage*.

4.4. Test 2: multi-harmonic disturbance

This second example aimed to supply further proof of the concept that optimal vibration control does not correspond to optimal fatigue damage control. The test configuration is consistent with that presented in the previous sections, considering the FRF and Rainflow tests for the NC, LQR and FLQR systems. In this case the disturbances are represented by the sum of two harmonics having the same amplitude and different frequencies, $f_1 = 10.5$ Hz and $f_2 = 48.1$ Hz. Both of them excite the system around a resonance, more precisely the 1st and the 9th resonances. For the reasons explained above, the higher frequency disturbance induces greater fatigue damage on the structure. Therefore, the adaptive logic concentrates the greatest control effort on the ninth mode.

Table 1
Cumulative structure damage on a $\Delta T = 300$ s time history for the Not Controlled (NC) System, and LQR and FLQR controlled system for a $[0, 50]$ Hz Random Disturbance (test 1).

	NC	LQR	FLQR
Max damage (%)	9.40e−5	1.45e−6	5.56e−7
Mean damage (%)	3.21e−5	4.96e−7	2.23e−7
Max damage reduction (%)		98.46	61.63
Mean damage reduction (%)		98.46	54.98

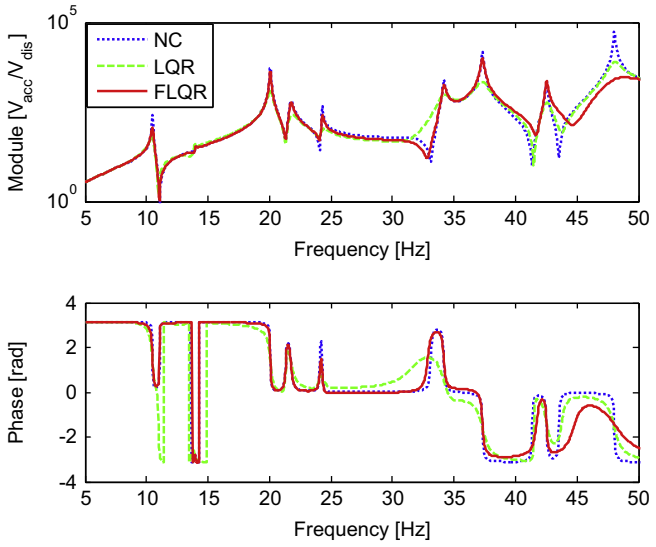

Fig. 8. Numerical FRF between the disturbance piezoelectric patch IV and accelerometer 8 for the following configurations: NC, LQR and FLQR for 10.5 Hz and 48.0 Hz harmonic disturbances (test 2).

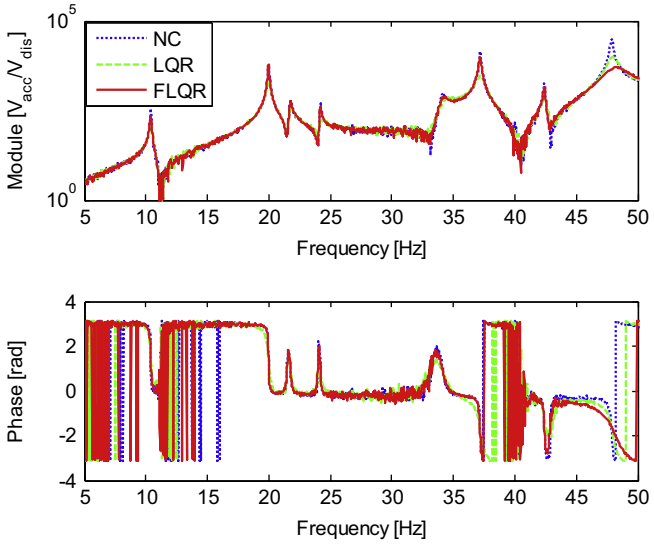

Fig. 9. Experimental FRF between the disturbance piezoelectric patch IV and accelerometer 8 for the following configurations: NC, LQR and FLQR for 10.5 Hz and 48.0 Hz harmonic disturbances (test 2).

Table 2
Cumulative structure damage on a $\Delta T = 300$ s time history for the Not Controlled (NC) System, and LQR and FLQR controlled system for a [0, 50] Hz harmonic disturbances (test 2).

	NC	LQR	FLQR
Max damage (%)	1.16e−4	2.41e−6	4.59e−7
Mean damage (%)	4.76e−5	9.50e−7	2.14e−7
Max damage reduction (%)		97.92	80.95
Mean damage reduction (%)		98.00	77.47

The numerical and experimental FRF (Figs. 8 and 9) show that FLQR control (adapted for this disturbance condition) is stronger than LQR control on the ninth mode. A relaxation on the first mode is also present. This is because the control logic perceives the ninth mode as the most dangerous for structure fatigue life (higher stress and higher frequency).

The benefits of this control logic are shown by the fatigue damage reduction for the FLQR logic that can be found in Table 2 and Rainflow histograms in Fig. 10.

5. Conclusions

The main objective of this research was to define a control law for smart structures integrating fatigue damage and vibration reduction. An in-depth analysis of the fatigue phenomenon in the frequency domain was presented, showing that fatigue damage:

- grows linearly with the structure vibration frequency;
- is nonlinear with the oscillation amplitude owing to the *S–N* curve shape and the equivalent stress criterion.

For these reasons the proposed control logic, denominated FLQR (Fatigue Linear Quadratic Regulator), was designed as an adaptive optimal control logic, which updates the control gains minimizing a quadratic formula that is a function of the measured modal vibration amplitude.

This control logic was compared with LQR and tested both numerically and experimentally. In particular, the experimentation was carried out on a thin carbon fibre epoxy plate, aiming to control the first 9 modes ([0, 50] Hz) and observing the first 15 ones ([0, 90] Hz). The results showed an interesting improvement in terms of structure fatigue damage both from the qualitative and quantitative points of view. Damage is reduced by one order of magnitude between the LQR and the FLQR controlled systems, with a consequent increase of structure lifetime.

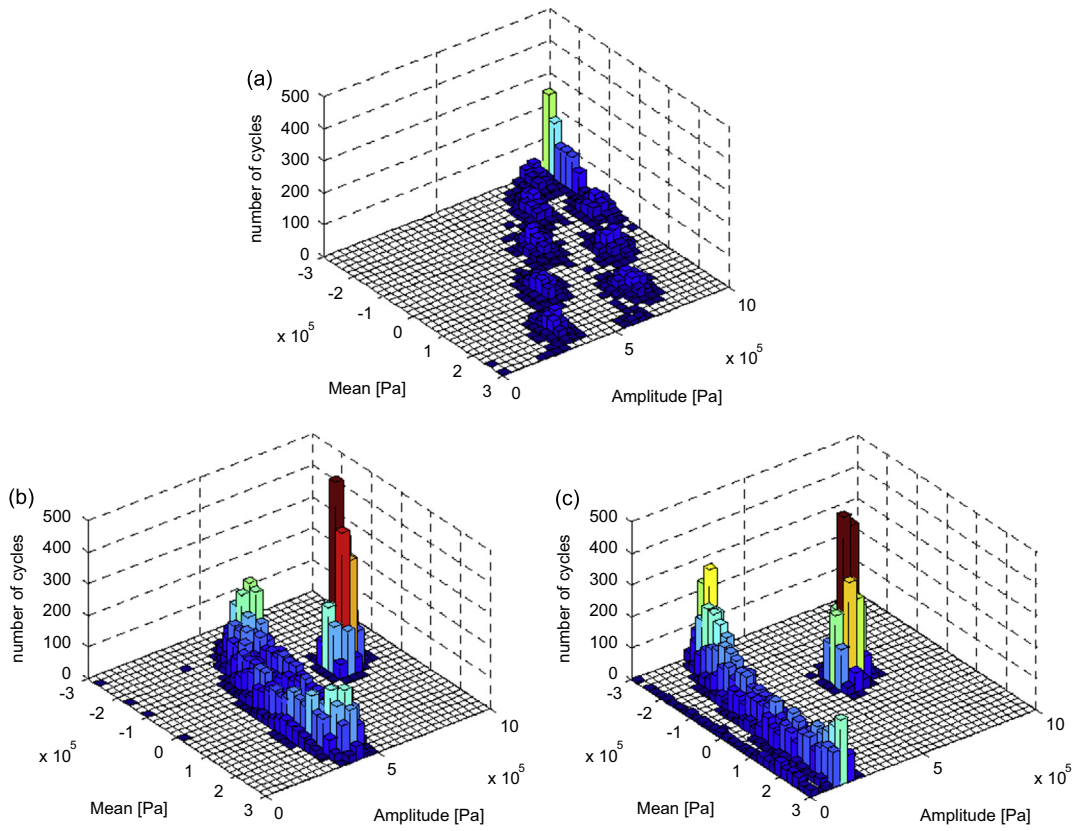

Fig. 10. Experimental Rainflow histogram (i.e. each bar represents the number of cycles associated to a certain amplitude and a mean value) for 10.5 Hz and 48.0 Hz harmonic disturbances (test 2) on NC (a), LQR (b) and FLQR (c) system.

References

[1] A. Ray, X. Dai, M. Carpino, C. Lorenzo, *Damage-Mitigating Control: An Interdisciplinary Thrust Between Controls and Material Science*, Vol. 3, IEEE, 1994.
[2] A. Golafshani, A. Gholizad, Passive vibration control for fatigue damage mitigation in steel jacket platforms, *International Journal of Engineering—Transactions B: Applications* 21 (4) (2008) 313.
[3] A.D. Wright, M.J. Balas, Design of controls to attenuate loads in the controls advanced research turbine, *Transactions of the ASME—Journal of Solar Energy Engineering* 126 (4) (2004) 1083–1091.
[4] E. Bossanyi, Wind turbine control for load reduction, *Wind Energy* 6 (3) (2003) 229–244.
[5] S.J. Johnson, S. Larwood, G. McNerney, C. Dam, Balancing fatigue damage and turbine performance through innovative pitch control algorithm, *Wind Energy* 15 (5) (2012) 665–677.
[6] B. Chomette, S. Chesn, D. Rmond, L. Gaudiller, Damage reduction of on-board structures using piezoelectric components and active modal control-application to a printed circuit board, *Mechanical Systems and Signal Processing* 24 (2) (2010) 352–364.
[7] G. Cazzulani, F. Resta, F. Ripamonti, A feedback and feedforward vibration control for a concrete placing boom, Journal of Vibration and Acoustics, *Transactions of the ASME* 133 (5) (2011) (art. no. 051002).
[8] J.W. Miles, On structural fatigue under random loading, *Journal of the Aeronautical Sciences* 21 (11) (1954) 753–762.
[9] P.C. Paris, The fracture mechanics approach to fatigue, in: 10th Sagamore Army Materials Research Conference, Syracuse University Press, 1964, pp. 107–132.
[10] R.E. Reed-Hill, A. Reza, *Physical Metallurgy Principles*, 3rd ed. PWS Publishing Company, Boston, 1994.
[11] A. Palmgren, Die lebensdauer von kugellagern, *Zeitschrift des Vereins Deutscher Ingenieure* 68 (14) (1924) 339–341.
[12] M. Miner, et al., Cumulative fatigue damage, *Journal of Applied Mechanics* 67 (12) (1945) 159–164.
[13] G. Sines, Behavior of metals under complex static and alternating stresses, *Metal Fatigue* 1 (1959) 145–169.
[14] R. Vinter, *Optimal Control*, Birkhäuser, Boston, 2010.
[15] B. Friedland, *Control System Design: An Introduction to State-space Methods*, Courier Dover Publications, 2012.
[16] C.C. Lee, Fuzzy logic in control systems: *fuzzy logic controller. I, IEEE Transactions on Systems Man and Cybernetics* 20 (2) (1990) 404–418.
[17] R.E. Kalman, et al., A new approach to linear filtering and prediction problems, *Journal of Basic Engineering* 82 (1) (1960) 35–45.
[18] R.E. Kalman, R.S. Bucy, New results in linear filtering and prediction theory, *Journal of Basic Engineering* 83 (3) (1961) 95–108.
[19] D. Revuelta, A. Miravete, Fatigue damage in composite materials, *International Applied Mechanics* 38 (2) (2002) 121–134.
[20] P. Reis, J. Ferreira, J. Costa, M. Richardson, Fatigue life evaluation for carbon/epoxy laminate composites under constant and variable block loading, *Composites Science and Technology* 69 (2) (2009) 154–160.
[21] M. Matsuishi, T. Endo, *Fatigue of Metals Subjected to Varying Stress*, Japan Society of Mechanical Engineers, Fukuoka, Japan, 1968, pp. 37–40.
[22] S.D. Downing, D. Socie, Simple rainflow counting algorithms, *International Journal of Fatigue* 4 (1) (1982) 31–40.
[23] A. Standard, E1049-85, Standard Practices for Cycle Counting in Fatigue Analysis, ASTM.